

First results from a second generation toroidal electron spectrometer.

L Broekman, A Tadich, E Huwald, J Riley, R Leckey
T Seyller*, K Emtsev*, L Ley*

Department of Physics, La Trobe University, Victoria 3086, Australia.

**Institut für Technische Physik II, Universität Erlangen-Nürnberg, Erwin-Rommel-Strasse 1, 91058 Erlangen, Germany.*

Abstract

A second generation toroidal electron spectrometer is briefly described and results presented that demonstrate its capabilities. Band structure measurements obtained from graphitised SiC(0001) and X-ray photoelectron diffraction results from Cu(111) and graphite are presented.

Key words: Angle resolved photoelectron spectroscopy, ARUPS, band structure, X-ray photoelectron diffraction, SiC(0001), Cu(111), graphite, Kikutchi, Bragg

Introduction.

Angle resolved photoemission in which photoelectrons are collected over the full hemisphere above a surface has proven to offer profound information about material surfaces. Employing UV light, near surface valence electrons are stimulated from states sensitive to the translational symmetry of the crystal and so display energy dispersion as a function of electron wave vector k . Intensity measured over this hemisphere as a function of energy thus provides a 3-dimensional map of electron momentum distributions. A slice of this map by means of a narrow window centred on the Fermi energy, for example will provide a direct image of the Fermi surface. Crystal band structure is similarly obtained by selecting slices along chosen symmetry directions.

With the use of light extending into the X-ray region localized core levels emit spherical waves that subsequently scatter and diffract from neighbouring atoms imparting information on the atomic environment of the photoemitters. Intensity distributions above approximately 500eV may be readily interpreted in terms of forward scattering; the result of electron focusing by ionic cores along nearest neighbour directions. Holographic inversions of diffraction data have been used with varying degrees of success [1, 2] for structural determinations. Forward scattering, however, is a hindrance to holography since it is a zero order diffraction effect that does not contain the required phase information. X-ray Photoelectron Diffraction (XPD) patterns that do not yield the necessary phase information may thus be more reliably interpreted as two-dimensional projections of a surface crystal lattice.

The analyser described here is a "second-generation" toroidal system of the display-type [3] capable of detecting with high resolution within an energy window whose width is approximately 8% of the pass energy simultaneously over 180° solid angle. Photoemission intensity is measured for each azimuthal rotation step of the sample

crystal to create a projection of the measurement hemisphere. Following a brief description of the design of this spectrometer, we present examples of valence band and XPD data sets which demonstrate the significant advantages of this instrument over and above the obvious advantage of decreased data collection times for any such display-type spectrometer.

Data collection with the Toroidal electron Analyser

In common with our previous design [4] the analyser as shown in Fig. 1 consists of an input lens whose purpose is twofold; to re-focus electrons from the sample at the entrance to the toroidal sector and to reduce their energy to match the selected pass energy of the sector. The output lens elements image the output focal plane of the sector onto a 75mm diameter chevron channelplate and phosphor detector and in addition serve to maximise the detection efficiency of the channelplate by raising the electron energy. A significant difference in the present design is that the previous conical slit at the output plane of the toroidal sector has been widened to form a radial energy window. Electron trajectories meet at the detector to form a radial arc centred at the mid-point of the channelplate. Electrons emitted from the sample in the horizontal plane lie on a circular arc whose radius depends on their precise energy and whose location around the arc is directly related to their (polar) angle of emission from the sample.

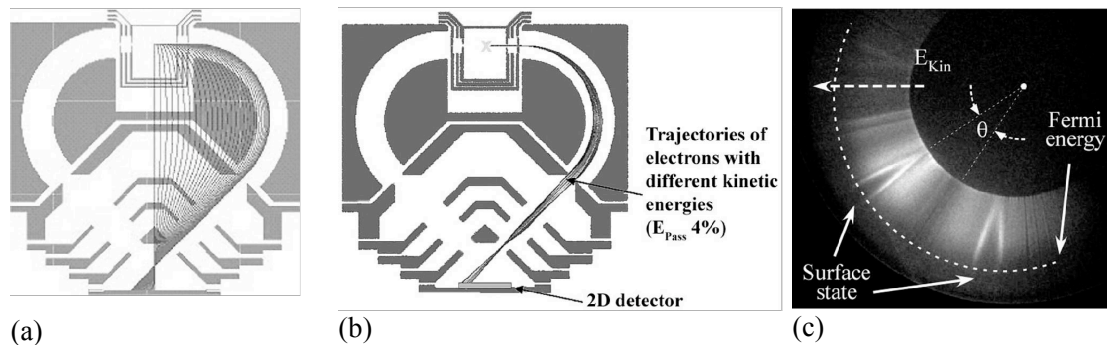


Fig. 1. Cross section of the toroidal analyser and lens elements as used to model electron trajectories showing; (a) 90° distribution of trajectories and (b) formation of a radial distribution of electron kinetic energies on the detector. (c) CCD image of the detector showing a window about the Fermi level of Cu_3Au . Kinetic energy, E_{kin} increases in the outwards radial direction, the surface state in the first and second Brillouin zone is also indicated.

Significant advantages follow from the use of this energy window. For example, in performing a standard azimuthal scan Fermi surface experiment, it is clearly necessary to select the "correct" Fermi energy in advance. With the present spectrometer a partial energy distribution is available at each emission angle thus allowing the Fermi level to be determined accurately once the data is acquired.

The detector consists of two 75mm channelplates coupled to a phosphor and a Quantix cooled CCD camera that images the complete emission arc. An example of a 600ms exposure obtained from the $\text{Cu}_3\text{Au}(111)$ surface exposed to 60eV photons and 10eV pass energy is shown as Fig 1. The window shows a 0.8eV slice of the photoelectron energy distribution in the neighbourhood of the Fermi energy. Clearly visible is the well known surface state emission close to the Γ point in the 1st and 2nd

Brillouin zones, together with emission from the s-p bands. The measurement azimuth, Γ -M in this case was determined from a previous survey azimuthal scan.

Intensity data is acquired by dividing the energy space visible within the window into arc segments whose energy separation is equal to the energy step size for the given experiment. Thus, each voltage step in an experiment corresponds to a window segment that can be added coherently to the last when building up an energy/angular intensity distribution.

Results

Graphite is a convenient test for a photoemission experiment since it is very close to an ideal 2-dimensional system thus alleviating the need to account for k_{\perp} in the interpretation of band structure in addition to the fact that it has a very well studied electronic structure. A well ordered graphitic layer displaying an excellent 1×1 LEED pattern of single crystal graphite was obtained by annealing SiC(0001) at about 1400°C in vacuum [6]. Energy Distribution Curves (EDC's) taken using p-polarized light at 35° incidence and oriented along two major symmetry directions may be compared to recently calculated band structure [5] in Fig.2 below.

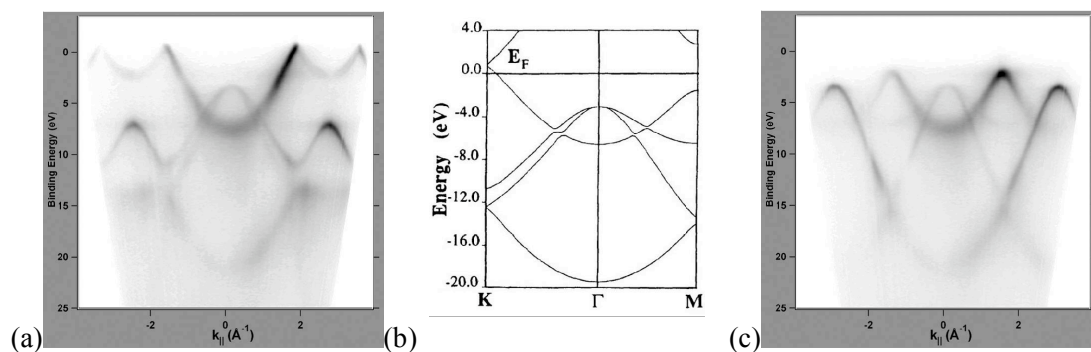


Fig. 2. EDC's taken from the Γ -K (a) and Γ -M (c) directions (60eV photon energy). Data is presented in its raw format except for the horizontal scale which has been converted to momentum, k_{\parallel} and intensity which has been inverted for clarity of presentation. (b) Calculated band structure [5] for simple hexagonal graphite along the relevant lines in the BZ shown.

XPD results obtained from both Cu(111) and the SiC(0001) graphite surfaces are shown in Fig. 4 below, the centre of these stereographic projections correspond to the surface normal $[111]$ direction. These XPD scans are constructed from $2\pi/3$ data sets since symmetrically equivalent regions within a full 2π scan are identical. Fig. 4(a) was taken at an energy for which forward scattering begins to dominate the intensity distribution [7] and clearly shows intensity bands corresponding to the low index crystal directions. For graphite (Fig. 4(b)) on the other hand the normally bright forward scattering features are less apparent compared to the curved bands which dominate this diffraction pattern. This may be expected for such low kinetic energies and the low scattering cross section for this low-Z material [8].

Also very clearly seen in both XPD patterns are a series of less commonly resolved dark semicircular extinction-lines. Kikuchi-like bands and extinction-lines resulting from Bragg reflections off crystal planes have been previously modelled [9]. X-ray photoelectron emission can be considered as coming from point sources embedded in the crystal and as a first approximation can be considered as homogeneous emitters.

Bragg scattering will reflect electrons impinging on crystal planes at the Bragg angle θ resulting in no propagation for a cone with apex angle of 2θ . The intersection of this cone with the surface plane is an ellipse seen as dark extinction-lines. Bragg reflection features are found to be quite sharp ($\theta < 1^\circ$ FWHM) the clarity of these features thus alludes to a high angular resolution for this instrument.

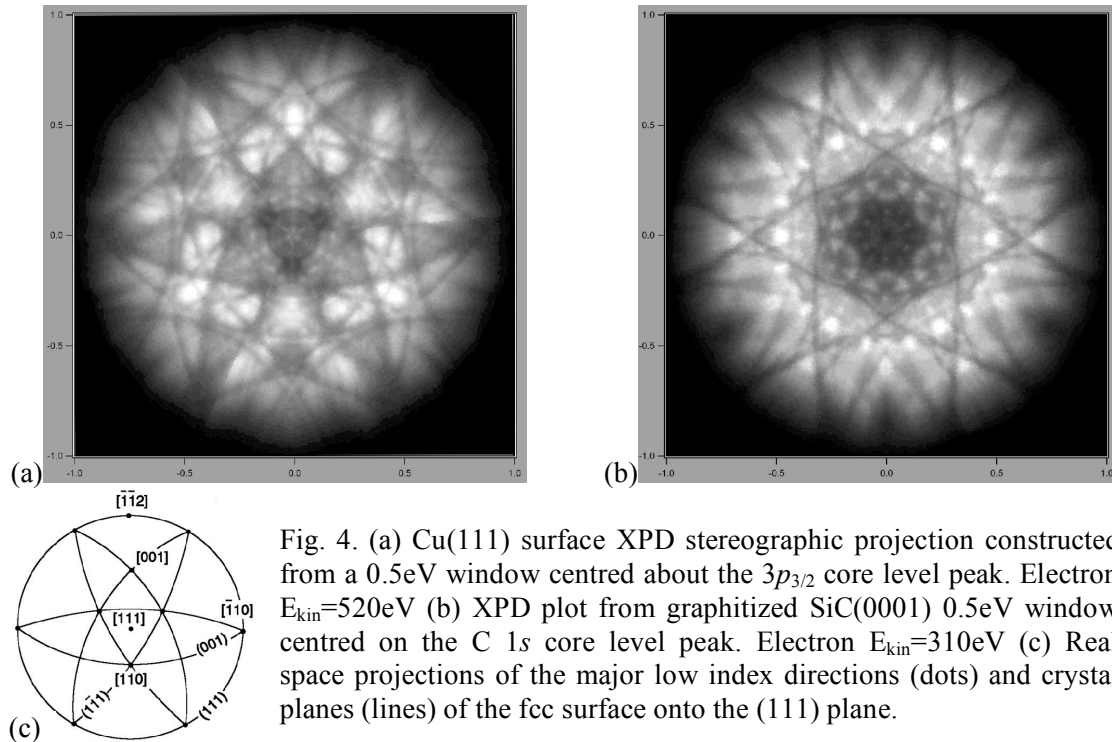


Fig. 4. (a) Cu(111) surface XPD stereographic projection constructed from a 0.5eV window centred about the $3p_{3/2}$ core level peak. Electron $E_{kin}=520\text{eV}$ (b) XPD plot from graphitized SiC(0001) 0.5eV window centred on the C 1s core level peak. Electron $E_{kin}=310\text{eV}$ (c) Real space projections of the major low index directions (dots) and crystal planes (lines) of the fcc surface onto the (111) plane.

In contrast to previously published XPD results from HOPG graphite [8] which display randomly oriented micro-crystalline material these results (fig. 4. (b)) again demonstrate that an exceptionally well ordered single crystal layer can be obtained from the graphitization of SiC(0001).

Conclusion

Preliminary results obtained from the Cu(111) and SiC(0001) graphitised surface using the second generation toroidal analyser demonstrate a functional instrument capable of obtaining angle resolved photo emission data quickly and with high angular resolution. Further experiments using a high energy resolution beamline is required before energy resolution limits can be ascertained.

Acknowledgements

We wish to acknowledge the Australian Research Counsel for there financial support.

References

- [1] Gobor, D Nature 161, 777 (1948)
- [2] Greber, T. J. Phys.: Condens. Matter **13**, 10561 (2001).
- [3] Greber, T *et al.* Rev. Sci. Instrum. **68**, 4549 (1997)
- [4] Leckey, R. C. G. Riley, J. D. Appl. Surf. Sci. **22/23**, 196 (1995)
- [5] Charlier, J.C. Michenaud, J.P. Gonze, X. Phys. Rev. B. **46**, 4531 (1992)
- [6] Forbeaux, I. Themlin, J.M. Debever, J.M. Phys. Rev B. **58**, 16396 (1998)
- [7] Osterwalder, J. *et al.* Surf. Sci. **331-333**, 1002 (1995)
- [8] Küttel, O. Agostino, R. Fasel, R. Osterwalder, L. Schlapbach, L. Surf. Sci. **312**, 131 (1994)
- [9] Trehan, R. Osterwalder, J. Fadley, C. S. J. Elec. Spec. Rel. Phen. **42**, 187 (1987)